

ARTICLE

## Integration of GIS with the Generalized Reciprocal Method (GRM) for Determining Foundation Bearing Capacity: A Case Study in Opolo, Yenagoa Bayelsa State, Nigeria

Ebiegberi Oborie<sup>\*</sup> , Desmond Eteh<sup>†</sup> 

Department of Geology, Niger Delta University, Wilberforce Island, Bayelsa State, 560103, Nigeria

### ABSTRACT

This study addresses the pressing need to assess foundation bearing capacity in Opolo, Yenagoa, Bayelsa State, Nigeria. The significance lies in the dearth of comprehensive geotechnical data for construction planning in the region. Past research is limited and this study contributes valuable insights by integrating Geographic Information System (GIS) with the Generalized Reciprocal Method (GRM). To collect data, near-surface seismic refraction surveys were conducted along three designated lines, utilizing ABEM Terraloc Mark 6 equipment, Easy Refract, and ArcGIS 10.4.1 software. This methodology allowed for the determination of key geotechnical parameters essential for soil characterization at potential foundation sites. The results revealed three distinct geoseismic layers. The uppermost layer, within a depth of 0.89 to 1.50 meters, exhibited inadequate compressional and shear wave velocities and low values for oedometric modulus, shear modulus, N-value, ultimate bearing capacity, and allowable bearing capacity. This indicates the presence of unsuitable, soft, and weak alluvial deposits for substantial structural loads. In contrast, the second layer (1.52 to 3.84 m depth) displayed favorable geotechnical parameters, making it suitable for various construction loads. The third layer (15.00 to 26.05 m depth) exhibited varying characteristics. The GIS analysis highlighted the unsuitability of the uppermost layer for construction, while the second and third layers were found to be fairly competent and suitable for shallow footing and foundation design. In summary, this study highlights the importance of geotechnical surveys in Opolo's construction planning. It offers vital information for informed choices, addresses issues in the initial layer, and suggests secure, sustainable construction options.

**Keywords:** Generalized reciprocal method (GRM); Geographic information system (GIS); Foundation bearing capacity; Seismic refraction

#### \*CORRESPONDING AUTHOR:

Ebiegberi Oborie, Department of Geology, Niger Delta University, Wilberforce Island, Bayelsa State, 560103, Nigeria; Email: ebix114@gmail.com

#### ARTICLE INFO

Received: 16 September 2023 | Revised: 23 October 2023 | Accepted: 25 October 2023 | Published Online: 15 November 2023  
DOI: <https://doi.org/10.30564/agger.v5i4.5969>

#### CITATION

Oborie, E., Eteh, D., 2023. Integration of GIS with the Generalized Reciprocal Method (GRM) for Determining Foundation Bearing Capacity: A Case Study in Opolo, Yenagoa Bayelsa State, Nigeria. *Advances in Geological and Geotechnical Engineering Research*. 5(4): 22-40. DOI: <https://doi.org/10.30564/agger.v5i4.5969>

#### COPYRIGHT

Copyright © 2023 by the author(s). Published by Bilingual Publishing Group. This is an open access article under the Creative Commons Attribution-NonCommercial 4.0 International (CC BY-NC 4.0) License. (<https://creativecommons.org/licenses/by-nc/4.0/>).

# 1. Introduction

The assessment of foundation bearing capacity holds a pivotal role in the planning and execution of diverse civil engineering projects, encompassing the construction of buildings, bridges, and various infrastructural undertakings [1,2]. The stability of any structure firmly hinges on the soil's appropriateness for a foundation. The utilization of compressible soil in foundation construction often leads to subsidence issues, thereby underscoring the critical need for an accurate evaluation of soil characteristics to ensure the stability and long-term functionality of these structures [3,4]. Traditionally, geotechnical investigations have heavily relied on invasive techniques like boreholes and laboratory tests to amass data indispensable for foundation design [5]. Nevertheless, these approaches can be labor-intensive and cost-prohibitive, and may not furnish a comprehensive comprehension of subsurface conditions [6,7]. In recent years, the integration of Geographic Information System (GIS) methods with geotechnical engineering has emerged as a potent instrument for site characterization and foundation design [8]. GIS offers an efficient means of organizing, visualizing, and analyzing geospatial data, thereby empowering engineers to make well-informed decisions grounded in precise and current information [9]. One notable application of GIS in geotechnical engineering involves the utilization of the Generalized Reciprocal Method (GRM) for the determination of foundation bearing capacity. The Generalized Reciprocal Method (GRM) constitutes a non-invasive geophysical approach widely employed in seismic refraction surveys [10]. It serves the purpose of establishing the seismic velocity structure of subsurface materials, which is invaluable information in a myriad of geophysical and engineering contexts, including site characterization, geological mapping, and the assessment of bedrock depth or other geological strata. Through the estimation of shear wave velocity, engineers can gauge the soil's stiffness, and by extension, its bearing capacity [11]. Yenagoa, the capital city of Bayelsa State in Nigeria, has undergone a rapid process of urbanization and

witnessed a substantial upsurge in its population in recent years. Consequently, there exists an escalating demand for the development of infrastructure, encompassing the construction of residential, commercial, and public edifices [12]. Nevertheless, the region grapples with intricate geological and geotechnical conditions that pose substantial challenges for foundation design. This case study is specifically geared towards the application of GIS techniques and the Generalized Reciprocal Method (GRM) for the assessment of foundation bearing capacity in Yenagoa, Bayelsa State, Nigeria. The study area is marked by a heterogeneous geological composition, encompassing soft clay, silt, and sand deposits, each of which can exert a significant influence on the mechanical properties of the soil and, consequently, its bearing capacity.

### Study area

The focus of our investigation is Opolo, situated in Yenagoa, the capital city of the south-south geopolitical region of Nigeria. Opolo is a swiftly developing urban area within this region [2]. Our study encompasses an area of approximately 170 square kilometers and benefits from a well-developed road network that links various parts of Yenagoa city and its environs. This particular zone can be pinpointed between longitudes 006°14'30" and 006°21'30" east of the prime meridian and latitudes 04°55'0" and 05°0'30" north of the equator, positioned in the coastal region of the Niger Delta (see **Figure 1**).

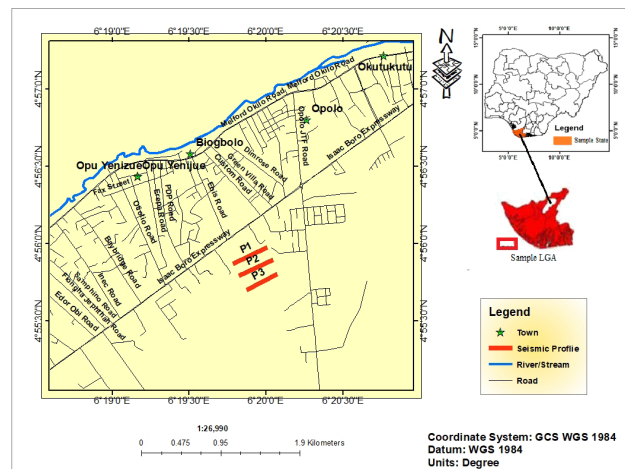


Figure 1. Map of the study area.

## 2. Materials and methods

### 2.1 Materials

ABEM Terraloc Mark 6 A sledgehammer and metal plate; a group of 12 vertical geophones at 14 Hz; seismic cable reels; Wire reel, 12-volt DC battery, log book, Global Positioning System device (GPS), measuring tape.

### 2.2 Methods

#### *Seismic refraction*

Seismic refraction is a geophysical method that entails the measurement of the time it takes for seismic waves to propagate through different underground layers of the Earth's crust<sup>[13]</sup>. This technique is of utmost importance in aiding engineers and geologists in acquiring a deeper understanding of the geological features and characteristics beneath the Earth's surface. The data gathered from seismic refraction surveys holds significant value for a diverse set of purposes, including but not limited to foundation design, site assessment, and geotechnical engineering<sup>[2,14]</sup>.

#### *Generalized reciprocal method (GRM)*

The Generalized Reciprocal Method (GRM) is a mathematical approach employed in seismic refraction surveys for the determination of subsurface velocity profiles and the depths of different geological layers<sup>[15]</sup>. Seismic refraction surveys are commonly employed to investigate subsurface geology, aiming to ascertain the characteristics and depths of various geological strata, like bedrock and sedimentary deposits<sup>[10]</sup>. The GRM serves as an extension of the conventional seismic refraction method, proving particularly valuable when dealing with intricate subsurface structures characterized by irregular layer boundaries or variations in lateral velocity<sup>[16]</sup>. It enables geophysicists to enhance the precision of their interpretations of subsurface conditions by accounting for these complexities. Nevertheless, it necessitates meticulous data collection and analysis, and the outcomes are typically presented in the form of velocity-depth models, offering valuable insights

into the geological attributes at a specific location.

#### *Seismic data acquisition*

Seismic refraction was conducted in an undeveloped area, involving three profiles surveyed using the 12-channel ABEM Terraloc Mark 6. The equipment included the seismograph, geophones, a 15 kg sledgehammer, measuring tapes, and more. Profiles spanned 75 m, with geophones placed 5 m apart to capture accurate data and depth details. The study area's isolation from noise sources like traffic and human activity enhanced data quality. Seismic waves were generated using a sledgehammer and detected by geophones, with both P-waves and S-waves recorded using 14-Hz geophones. Five stacks were produced per shot location, capturing critically refracted waves. The refracted energy was converted into digital signals and stored in memory. The research encompassed three profile lines, each 75 m long, marked by GPS for accurate geophone and shot position data using the generalized reciprocal method (GRM). The method allowed for imaging subsurface boundaries based on seismic wave behavior.

#### *Data processing*

The utilization of Easy Refract and ArcGIS software version 10.5 for handling the data. The result of this data manipulation unveiled valuable subsurface characteristics, which served as vital inputs for geotechnical and engineering evaluations in various projects (as shown in **Figures 2a to 2i**). Additionally, a spatial distribution map was generated to visually represent the geographical spread of the data. This comprehensive analysis greatly assists decision-making in the fields of geotechnical and engineering endeavors.

The GRM process can be outlined as follows:

- 1) Manual identification of initial arrivals, either through direct entry or copy-paste commands. **Figures 2a-2e** display the selected first arrival times from collected wave records.

- 2) Custom definition of time travel curves, achieved by drawing lines through the selected first arrival times or by utilizing software to fit a curve to the data. The outcome of this step is demonstrated in

**Figure 2f.**

3) Automated detection of slope change points on the time travel curves, performed with the assistance of software to identify the points where the slope changes.

**Figure 2g** illustrates the results of this stage.

4) Selection of the optimal XY value on the velocity function diagram. The velocity function is a plot of refractor velocity against XY distance. The optimal XY value is where the velocity function is most stable and exhibits the fewest changes, as shown in **Figure 2h**.

5) Selection of the optimal XY value on the time-depth function diagram. The time-depth function displays the depth of the refractor against XY distance. The optimal XY value is the one where the time-depth function is smoothest and provides the most detail, as depicted in **Figure 2i**.

After determining the optimal XY value, you can calculate the depth to the refractor at any point along the survey line using the following equation:

$$\text{Depth} = (XY/2) * (1/\text{Velocity}) \tag{1}$$

where:

- Depth represents the depth to the refractor in meters.
- XY is the preferred XY distance in meters.
- Velocity is the refractor velocity in meters per second.

The GRM is a robust and versatile seismic refraction technique used to obtain precise and detailed information about subsurface conditions. It finds application in various fields, including engineering and geotechnical investigations, groundwater exploration, mineral exploration, and environmental assessments.

**Table 1** holds a pivotal position in understanding the properties of P-waves, S-waves, and a variety of geotechnical parameters. It not only furnishes precise definitions but also encompasses the mathematical expressions associated with primary, shear wave, and geotechnical properties.

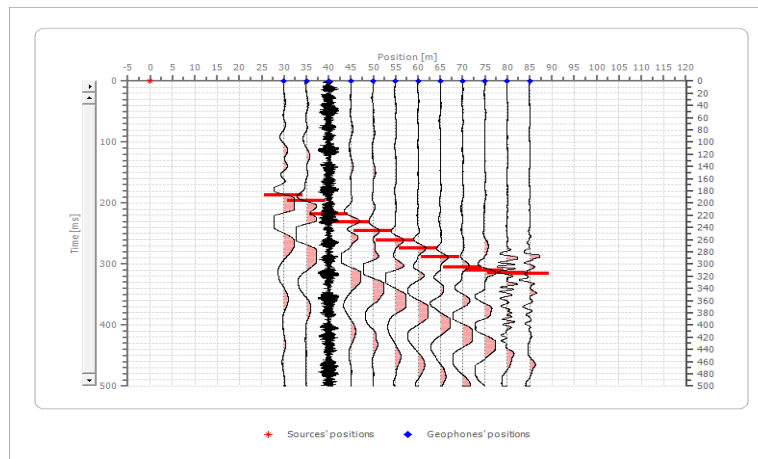


**Figure 2a.** A sample of a picked first wave arrival time from the collected wave records at 0 m.

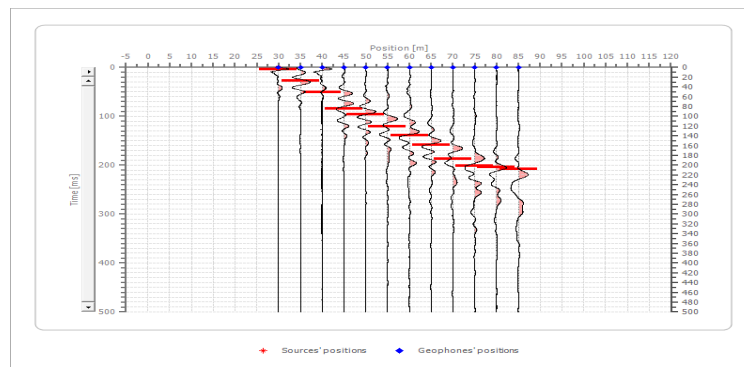


**Figure 2b.** A sample of a picked first wave arrival time from the collected wave records at 30 m.

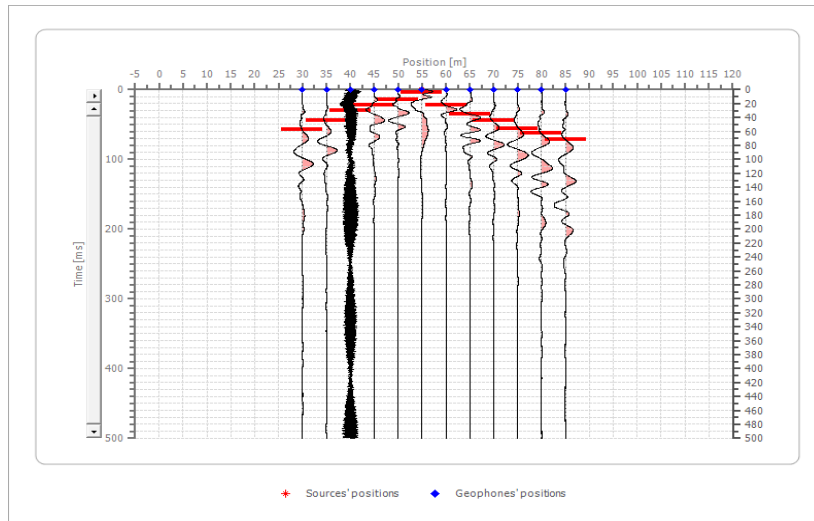


Figure 2c. A sample of a picked first wave arrival time from the collected wave records 55 m.

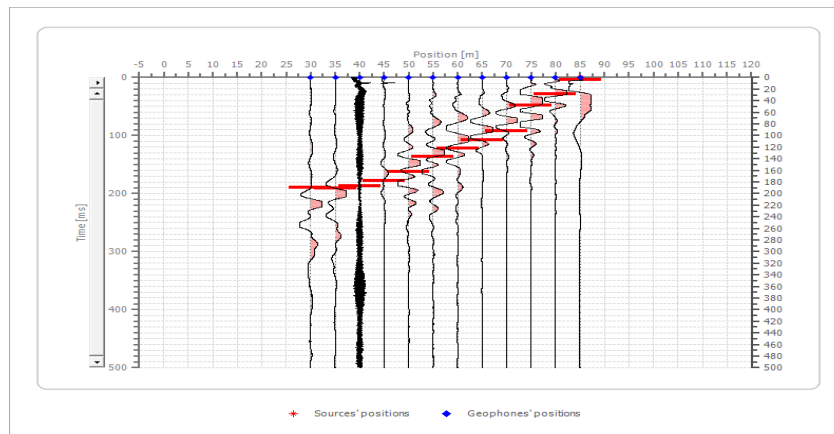


Figure 2d. A sample of a picked first wave arrival time from the collected wave records at 85 m.

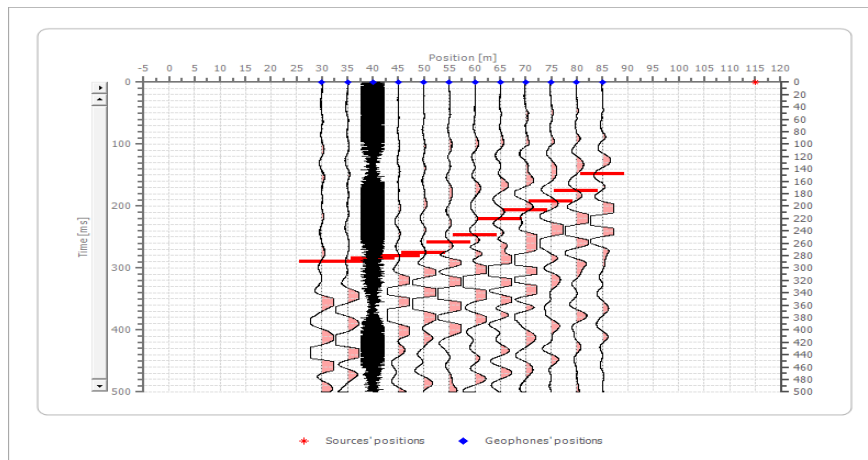


Figure 2e. A sample of a picked first wave arrival time from the collected wave records at 115 m.

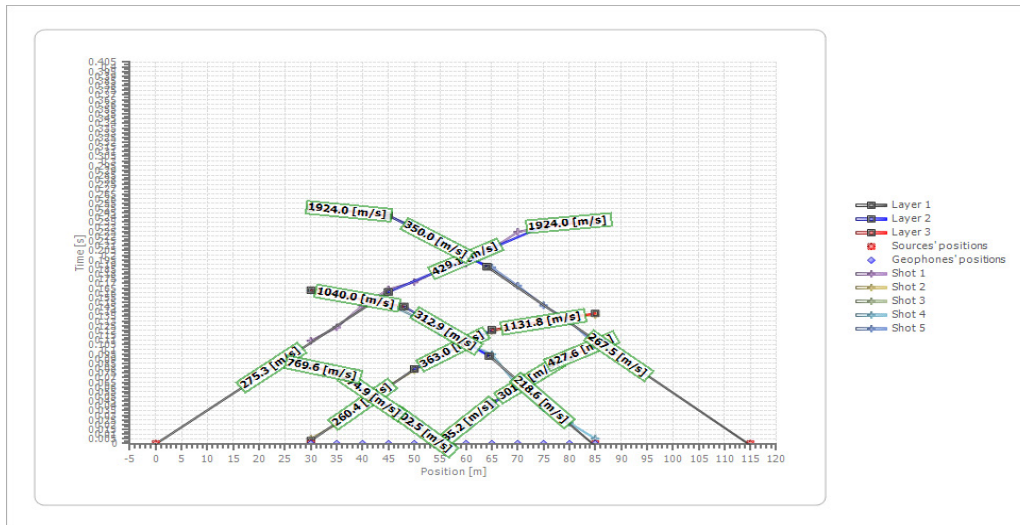


Figure 2f. Time travel curves.

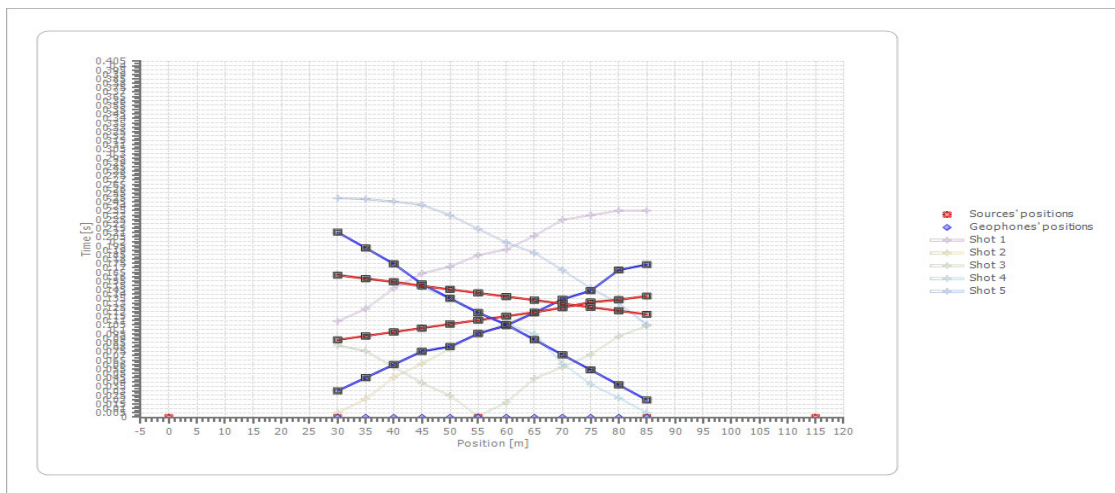


Figure 2g. Slope change points.

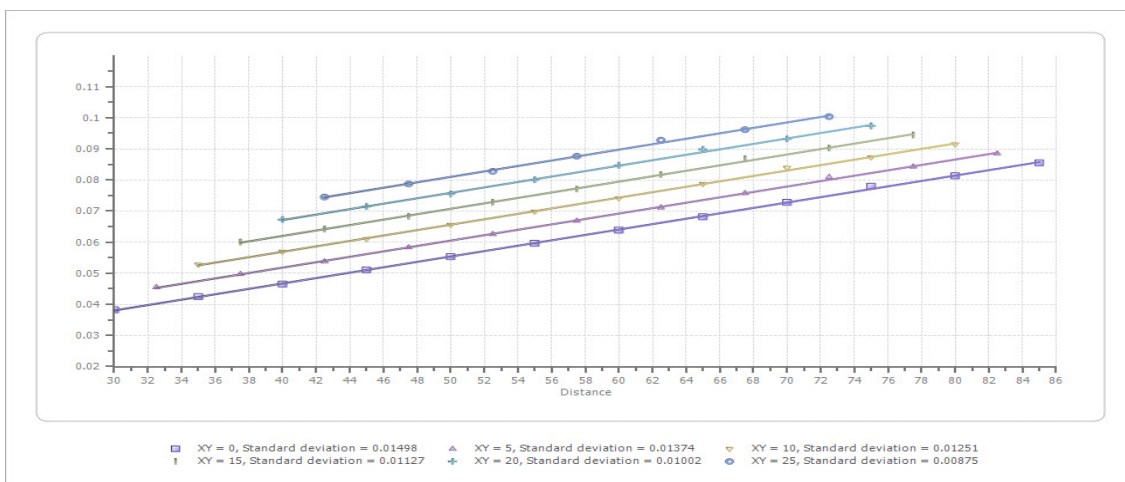


Figure 2h. Velocity function.

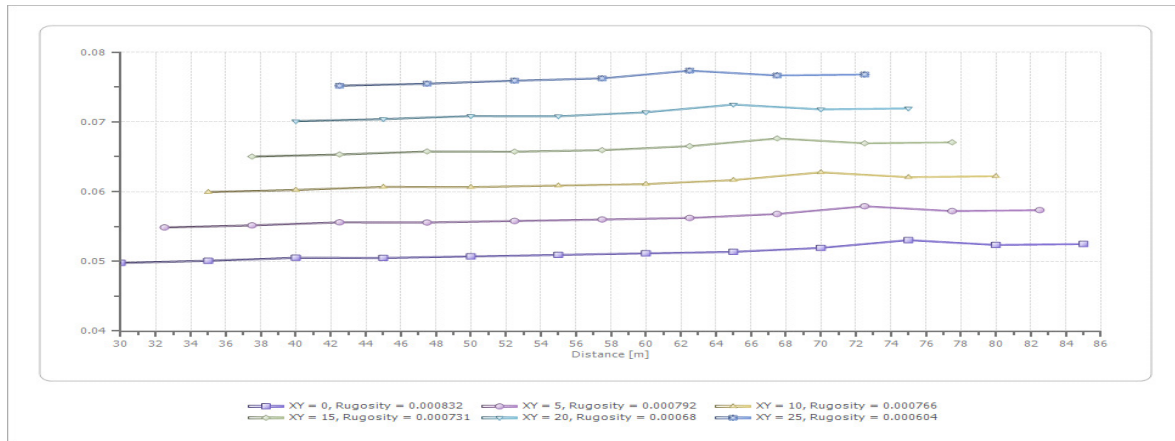


Figure 2i. Time-depth function.

### Spatial analysis using kriging interpolation

GIS provides spatial analysis, visualization, and data management, helping engineers and geologists assess site suitability, predict geological risks, and optimize infrastructure design. This synergy improves project efficiency, reduces costs, and minimizes environmental impacts, ensuring safer and more sustainable outcomes. Therefore, kriging claims that the distance or direction between the sampling points can be used to explain the surface variation. This involves exploratory statistical data analysis, simulation of variograms, surface creation and discovery of layers of variance (possibly). If you know that the data involves a spatially-based distance or directional bias, Kriging is more suitable. Kriging interpolation is mostly used in geology, geophysics and soil science. The GIS application was used to analyze all data layers through the process called “Overlay”. The spatial strategy consists of using a thematic scheme to apply Index Overlay to overlay one layer to another, thereby creating a new layer. In this analysis, different value scores were assigned to the map classes produced on each added map, and different weights were given to the maps [17]. In the selection site suitability for foundation in the study area, this approach has identified and resolved multi-criteria problems. Kriging believes that a spatial comparison can be used to describe the surface variability by the distance or direction between the

sampling points. Kriging is the weights of the relevant calculated values to achieve a forecast for an unknown position.

The formula of the kriging interpolators is the weighted sum of the data:

$$\hat{Z}(s_0) = \sum_{i=1}^N \lambda_i Z(s_i) \quad (2)$$

where:

$Z(s_i)$  = measured value at the  $i$ th location

$\lambda_i$  = an unknown weight for the measured value at the  $i$ th location

$s_0$  = Prediction location

$N$  = Number of measured values

### Geotechnical parameters

The provided **Table 2** presents a range of geotechnical parameters and their corresponding soil descriptions. These parameters have been sourced from various authors and studies [31-36].

**Table 3** shows the conventional p-wave velocities associated with various soil classifications as described by Nwankwoala and Amadi in their [37]. This table includes statistics on typical p-wave velocities for various soil types, acting as a resource for researchers and experts in the field. As stated by Nwankwoala and Amadi [37], it incorporates crucial information regarding the p-wave velocities of diverse soil kinds, providing a thorough knowledge of soil properties and assisting in geotechnical and seismic studies.

**Table 1.** Definition of primary, shear wave and geotechnical parameters.

Parameter	Definition	Formula	Citations
Primary wave velocity (P-wave) (m/s)	Propagate through the medium faster than other forms of waves and P waves often called compression waves or longitudinal waves	$V_p = \sqrt{\frac{k + \frac{4}{3}\mu}{\rho}}$ (K) Bulk modulus, ( $\mu$ ) Shear modulus, and ( $\rho$ ) density.	[18,19,20]
Secondary wave velocity (S-wave) (m/s)	The shear or transverse wave which propagates more slowly through a medium than the primary wave.	$V_s = \sqrt{\mu/\rho}$ $V_p \approx 1.7V_s$	[21,18,19,20]
Bulk density ( $\rho$ ) (kg/m <sup>3</sup> )	The mass of soil per unit volume	$P = \gamma/g$ $\gamma$ is the acceleration due to gravity = 9.8 m/s <sup>2</sup> .	[22,23]
Poisson's ratio ( $\sigma$ )	The ratio of lateral strain to axial strain in a material	$\text{Poisson's } (\sigma) = \frac{1}{2} \left[ 1 - \frac{1}{(V_p/V_s)^2 - 1} \right]$	[21,19]
Young's modulus (E) (Mpa)	The measure of stiffness of a material	$E = 2\mu(1 + \sigma)$	[24]
Oedometeric modulus (Ec) (Mpa)	The measure of stiffness of soil under one-dimensional compression	$E_c = \frac{(1 - \sigma)E}{(1 + \sigma)(1 - 2\sigma)}$	[25]
Bulk modulus (K) (Mpa)	The measure of a material's resistance to uniform compression	$K = \frac{E}{3(1 - 2\sigma)}$	[26]
Shear modulus ( $\mu$ ) (Mpa)	The measure of a material's resistance to shear deformation	$\mu = \frac{\sigma E}{(1 + \sigma)(1 - 2\sigma)}$	[27]
N-value (N)	A standardized measure of soil consistency and density	$N = \left( \frac{V_s}{76.55} \right)^{2.24719}$	[28,29]
Ultimate bearing capacity (Qult) (Kpa)	The maximum load a soil can withstand before failure	$Q_{ult} = \log(30N)$	[30]
Allowable bearing capacity (Qa) (Kpa)	The maximum load a soil can bear without exceeding the allowable settlement or deformation limits	$Q_a = Q_{ult}/F$ The factor of safety equals 2 and 3 for the cohesionless and cohesive soils, respectively. Also, (Qa) can be estimated by using shear wave velocity $\text{Log } Q_a = 2.932 \text{ Log } V_s - 4.553$ for soft soil	[31]

**Table 2.** Serves as a reference for classifying soils based on specific engineering and geotechnical characteristics.

Soil/Rock description parameters	Weak		Fair		Good
	Incompetent		Fairly competent		Competent
	Very soft	Soft	Fairly compacted	Moderately compacted	Compacted
Concentration index (Ci)	3.5-4.0	4.0-4.5	4.5-5.0	5.0-5.5	5.5-6.0
Material index (Mi)	< -0.6	-0.6-0.2	-0.2-0.2	0.2-0.6	0.6-1.0
Stress ratio (Si)	0.7-0.61	0.61-0.52	0.52-0.43	0.43-0.34	0.34-0.25
Bearing capacity (Qult) (Kpa)	0-50	50-100	100-550	550-5000	5000-8000
Reaction modulus (Rm) (Mpa)	0-10	10-30	30-1000	1000-4800	4800-6000
Poisson's ratio	0.4-0.49		0.35-0.27	0.25-0.16	0.12-0.03

Table 3. Standard p-wave velocities for different soil types.

Rock/soil types	P-wave velocity (m/s)
Top soil	100-250
Sandy clay	300-500
Sand with gravel(dry)	500-700
Sand with gravel (wet)	700-1150
Coarse sand (wet)	1150-2000
Clay	1500-4200
Sandstone	1400-4300
Loose sand	1500-2000

Source: [37].

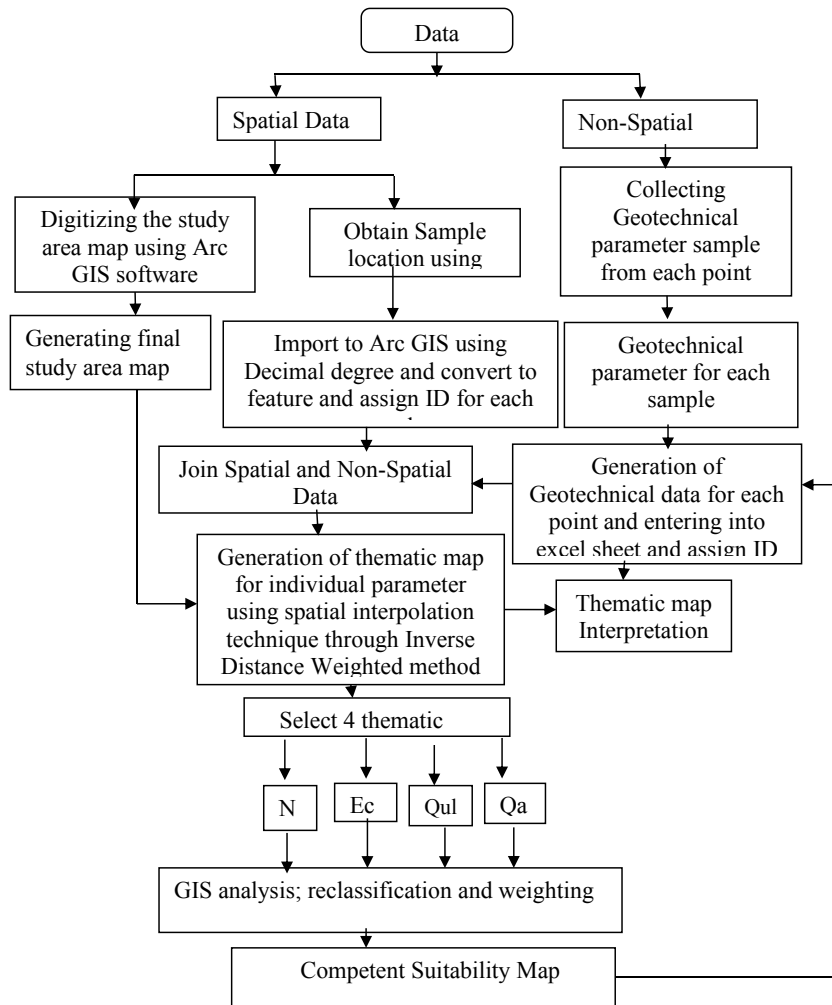


Figure 2j. Flow diagram.

### 3. Results and discussion

#### 3.1 Results

**Table 4** provides essential data related to seismic velocities in three different layers. This data is critical for assessing the foundation bearing capacity, which is crucial for construction and infrastructure development.

##### *Seismic velocities*

Seismic velocities are fundamental in understanding the subsurface geology and, in turn, the bearing capacity of the soil. The table provides seismic velocity data for the following parameters in three different layers (Layer I, Layer II, and Layer III):

- **Thickness (m):** This parameter represents the thickness of each layer. Layer I has a minimum thickness of 0.89 m, a maximum of 1.48 m, and a mean thickness of 1.162 m. Layer II and Layer III have similar statistics.

- **Primary Velocity (Vp) (m/s):** Primary velocity values vary across the layers. Layer I has a minimum of 236.2 m/s, a maximum of 264.4 m/s, and a mean value of 248.9 m/s. Layer II and Layer III exhibit similar trends.

- **Shear Velocity (Vs) (m/s):** Similar to primary velocity, shear velocity shows variation across the layers. Layer I has a minimum of 138.9 m/s, a maximum of 155.5 m/s, and a mean value of 146.38 m/s. Layer II and Layer III follow a similar pattern.

##### *Foundation bearing capacity*

**Table 4** also provides data on the foundation bearing capacity of each layer, as determined by the following parameters:

- **Unit Weight of the Soil (Y) (kgN/m<sup>3</sup>):** Unit weight, which represents the density of the soil, shows variation among the layers. Layer I has a minimum of 16.47 kgN/m<sup>3</sup>, a maximum of 16.53 kgN/m<sup>3</sup>, and a mean value of 16.498 kgN/m<sup>3</sup>. Layer II and Layer III display similar trends.

- **Bulk Density (ρ) (kg/m<sup>3</sup>):** Bulk density, which is another measure of soil density, exhibits variation. Layer I has a minimum of 1.681 kg/m<sup>3</sup>, a maximum of 1.687 kg/m<sup>3</sup>, and a mean value of 1.6836 kg/m<sup>3</sup>. Layer II and Layer III follow similar patterns.

- **Poisson's Ratio (σ):** Poisson's ratio remains

constant across all layers, indicating that this parameter does not vary with depth.

- **Young's Modulus (E) (Mpa):** Young's modulus shows variation among the layers, with Layer I having a minimum of 0.08 Mpa, a maximum of 0.101 Mpa, and a mean value of 0.0894 Mpa. Layer II and Layer III exhibit similar trends.

- **Oedometric Modulus (Ec) (Mpa):** Similar to Young's modulus, Oedometric modulus varies across the layers. Layer I has a minimum of 0.094 Mpa, a maximum of 0.118 Mpa, and a mean value of 0.1048 Mpa. Layer II and Layer III follow a similar pattern.

- **Bulk Modulus (K) (Mpa):** Bulk modulus exhibits variation among the layers, with Layer I having a minimum of 0.051 Mpa, a maximum of 0.064 Mpa, and a mean value of 0.0568 Mpa. Layer II and Layer III display similar trends.

- **Shear Modulus (μ) (Mpa):** Shear modulus varies among the layers, with Layer I having a minimum of 0.033 Mpa, a maximum of 0.041 Mpa, and a mean value of 0.0364 Mpa. Layer II and Layer III exhibit similar trends.

- **Concentration Index (Ci):** Concentration index remains constant across all layers, indicating a consistent level of soil concentration.

- **Stress Ratio (Si):** Stress ratio is also constant across all layers, suggesting a uniform stress level within the site.

- **Material Index (Mi):** Material index remains constant, indicating uniform material properties across the layers.

- **Reaction Modulus (Rm) (Mpa):** Reaction modulus shows variation across the layers, with Layer I having a minimum of 4.6112 Mpa, a maximum of 6.3286 Mpa, and a mean value of 5.37782 Mpa. Layer II and Layer III exhibit similar trends.

- **Ultimate Bearing Capacity (Qult) (Kpa):** Ultimate bearing capacity varies across the layers, with Layer I having a minimum of 114.5 Kpa, a maximum of 147.6 Kpa, and a mean value of 129.31 Kpa.

- **Allowable Bearing Capacity (Qa) (Kpa):** Allowable bearing capacity also varies among the layers. Layer I has a minimum of 57.249 Kpa, a maximum of 73.802 Kpa, and a mean value of 64.6552 Kpa.

**Table 4.** Seismic velocities of the investigated site as obtained from the refraction profiles and the corresponding calculated from **Table 1** for Minimum, maximum, mean values in Opolo.

Parameters	Layer I Opolo			Layer II Opolo			Layer III Opolo		
	Min	max	Mean	Min	max	Mean	min	max	mean
Thickness (m)	0.89	1.48	1.162	0.63	2.42	1.558	12.62	21	16.032
Primary velocity (Vp) (m/s)	236.2	264.4	248.9	421	471.6	449.68	1117	1153	1138.2
Shear velocity (Vp) (m)	138.9	155.5	146.38	247.6	277.4	264.5	657.1	678	669.46
Unit weight of the Soil (Y) (kgN/m <sup>3</sup> )	16.47	16.53	16.498	16.84	16.94	16.898	19.23	19.31	19.276
Bulk density (p) (kg/m <sup>3</sup> )	1.681	1.687	1.6836	1.719	1.729	1.7246	1.963	1.97	1.9672
Possion's ratio (σ)	0.235	0.235	0.235	0.235	0.235	0.235	0.235	0.235	0.235
Young's modulus (E) (Mpa)	0.08	0.101	0.0894	0.261	0.329	0.2994	2.094	2.238	2.179
Oedometeric modulus (Ec) (Mpa)	0.094	0.118	0.1048	0.305	0.385	0.3502	2.449	2.617	2.5482
Bulk modulus (K) (Mpa)	0.051	0.064	0.0568	0.164	0.207	0.1884	1.319	1.409	1.3722
Shear modulus (μ) (Mpa)	0.033	0.041	0.0364	0.105	0.133	0.1208	0.848	0.906	0.8822
Concentration index (Ci)	5.248	5.248	5.248	5.248	5.248	5.248	5.248	5.248	5.248
Stress ratio (Si)	0.308	0.308	0.308	0.308	0.308	0.308	0.308	0.308	0.308
Material index (Mi)	0.058	0.058	0.058	0.058	0.058	0.058	0.058	0.058	0.058
Reaction modulus (Rm) (Mpa)	4.6112	6.3286	5.37782	23.284	31.998	28.1982	385.22	391.06	388.424
N-value (N)	3.8163	4.9198	4.31016	13.99	18.054	16.2856	125.36	134.5	130.762
Ultimate bearing capacity (Qult) (Kpa)	114.5	147.6	129.31	460.15	541.63	504.76	3761	4034.6	3922.74
Allowable bearing capacity (Qa) (Kpa)	57.249	73.802	64.6552	230.08	270.81	252.38	1880.5	2017.3	1961.38

### 3.2 Discussion

#### Primary wave velocity

**Tables 4 and 5** at the specified location present profiles consisting of three distinct geoseismic layers. Within the first layer, P-wave velocities in Opolo are relatively low, ranging from 236.2 m/s to 264.4 m/s. This initial layer extends in depth from 0.89 m to 1.48 m in Opolo. These reduced velocities likely arise from the loose and soft nature of the soil, indicating lower elastic moduli and densities when compared to the values provided in **Table 3**<sup>[37]</sup>. At the Opolo site, the second layer exhibits velocities ranging from 421.00 m/s to 471.6 m/s, accompanied by layer thickness variations spanning from 0.63 m to 2.42 m. This suggests the presence of sandy clay in this layer, deviating from the standard P-wave velocities listed in **Table 3**. Moving on to the third geoseismic layer, observed exclusively at the Opolo sites, it displays higher velocities compared to the layers preceding it. In Opolo, velocities within this layer range from 1117 m/s to 1153 m/s, with depths ranging from 12 m to 21 m. This pattern suggests the presence of wet to coarse sand in this third layer. Spatial

distribution maps visually depict a transition in P-wave velocities, as indicated by blue areas in the first layer, shifting to increasing velocities represented by green, yellow, and red in the subsequent layers. **Figure 3** provides a graphical representation of this observed trend.

#### Shear wave velocity

The shear seismic wave velocity measurements obtained from the Opolo region exhibit distinct ranges for the first, second, and third geoseismic layers. For the initial layer, the velocities span 138.9 m/s to 155.5 m/s Opolo in **Tables 4 and 5**, indicating loose, unconsolidated sediments comprising surface soil and alluvial deposits. Conversely, the second layer displays higher shear wave velocities of 247.60 m/s to 277.40 m/s, suggesting more solid earth materials. The third layer, which marks the study's probing depth limit, showcases shear wave velocities ranging from 657.10 m/s to 678.00 m/s for Opolo. Spatially, Opolo's upper layer exhibits gradually increasing shear wave velocities from deep blue to white, while the second layer demonstrates a progressive velocity rise illustrated by colors transitioning from purple to red, as depicted in **Figure 4** below.

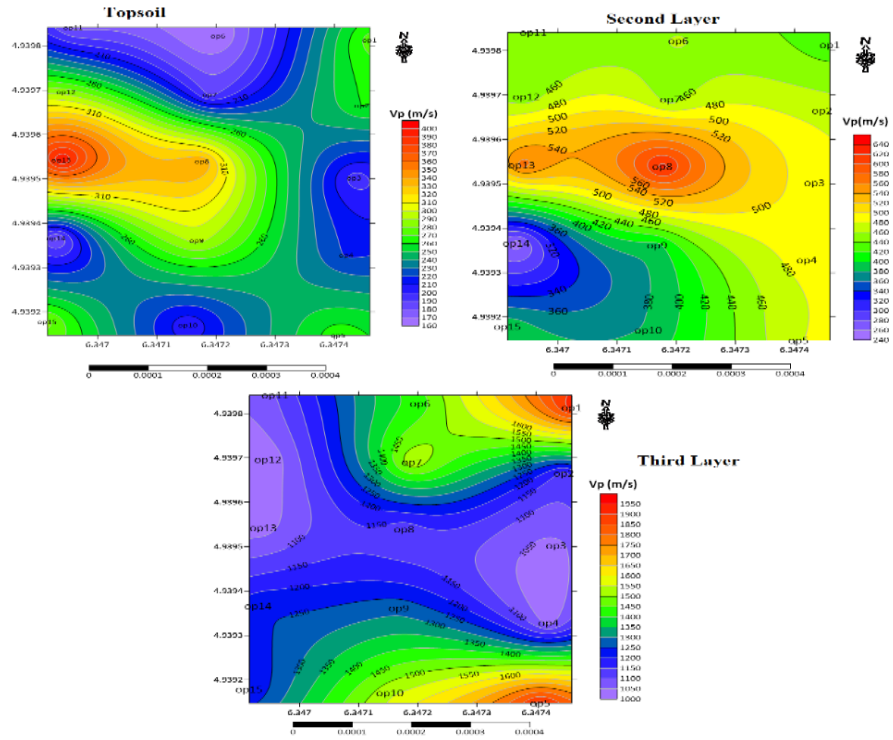


Figure 3. Distribution map of primary wave velocity in Opolo.

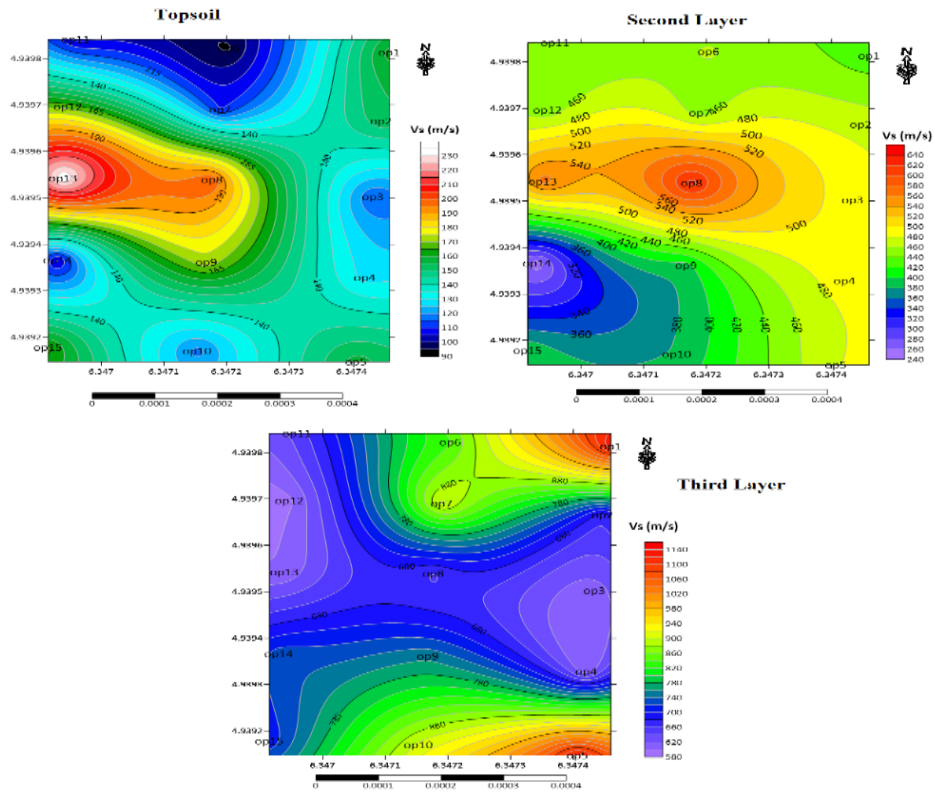


Figure 4. Distribution map of shear wave velocity in Opolo.

**Table 5.** Seismic velocities of the investigated site as obtained from five receiver geophones each in refraction survey and the corresponding calculated elastic moduli in Opolo.

Layer I Opolo								Layer II Opolo						Layer III Opolo					
Long	lat	Vp	Vs	Ec	N	Qult	Qa	Vp	Vs	Ec	N	Qult	Qa	Vp	Vs	Ec	N	Qult	Qa
6.34746	4.93981	275.3	161.941	0.1275	5.386	161.585	80.7923	429.1	252.4118	0.1275	5.386	161.585	80.7923	1924	1131.7647	7.2923	425.39	12761.4	6380.72
6.34745	4.93967	260.4	153.177	0.114	4.7529	142.594	71.2968	471.8	277.5294	0.114	4.7529	142.594	71.2968	1131.8	665.7647	2.523	129.109	3873.47	1936.73
6.34743	4.9395	194.5	114.647	0.0639	2.4786	74.3533	37.1766	489.4	287.8824	0.0639	2.4786	74.3533	37.1766	1040	611.7647	2.1306	125.916	4142.86	2071.43
6.34742	4.93933	218.6	128.588	0.0804	3.2077	96.2277	48.1138	488.7	287.4706	0.0804	3.2077	96.2277	48.1138	1029.3	605.4706	2.0794	106.758	5130.98	2565.49
6.34741	4.93915	267.5	157.353	0.1202	5.0491	151.461	75.7304	479	281.7647	0.1202	5.0491	151.461	75.7304	1924	1131.7647	7.291	425.39	12761.4	6380.72
6.3472	4.93982	160.3	94.2941	0.0433	1.5976	47.9292	23.9646	462.1	271.8235	0.0433	1.5976	47.9292	23.9646	1425.2	838.3529	4.001	214.988	6449.11	3224.56
6.34719	4.93969	186.99	109.994	0.0588	2.2582	67.733	33.8665	449.9	264.6471	0.0588	2.2582	67.733	33.8665	1539.2	905.4118	4.6663	257.639	7728.59	3864.29
6.34718	4.93954	339.06	199.447	0.1939	8.6014	258.048	129.024	628.28	369.5765	0.1939	8.6014	258.048	129.024	1119.26	658.3882	2.4588	125.916	3777.46	1888.73
6.34717	4.93936	293.9	172.882	0.1454	6.2383	187.37	93.685	392.8	231.0588	0.1454	6.2383	187.37	93.685	1282.7	754.5294	3.2411	171.042	5130.98	2565.49
6.34715	4.93917	200.6	118	0.0676	5.6444	79.3232	39.6616	382.92	225.2471	0.0676	5.6444	79.3232	39.6616	1539.2	905.4118	4.6663	257.639	7728.59	3864.29
6.34696	4.93984	176.4	103.765	0.0524	1.98	59.4292	29.7146	444.2	261.2941	0.0524	1.98	59.4292	29.7146	1099.5	646.7647	2.3814	120.976	3629.11	1814.55
6.34695	4.9397	285.5	167.941	0.137	5.8448	175.348	87.6738	447.3	263.1176	0.137	5.8448	175.348	87.6738	1012.7	595.7059	2.02	100.564	3017.17	1508.59
6.34694	4.93954	400.55	235.618	0.2706	12.5089	375.319	187.659	568.2	334.2353	0.2706	12.5089	375.319	187.659	1029.3	605.4706	2.0794	104.306	3128.96	1564.48
6.34693	4.93937	176.8	104	0.0526	1.991	59.731	29.8655	249.3	146.6471	0.0526	1.991	59.731	29.8655	1241.3	730.1765	3.0353	171.042	4766.5	2383.25
6.34692	4.93918	282.9	166.412	0.1345	5.7259	171.791	85.8954	396	232.9412	0.1345	5.7259	171.791	85.8954	1202.5	707.3529	2.848	257.639	4438.13	2219.06

### **Competent site suitability map for foundation**

The spatial distribution maps depicted in **Figures 5, 6, and 7** illustrate the variations in geotechnical parameters, namely oedometric modulus ( $E_c$ ), N-value, ultimate bearing capacity ( $Q_{ult}$ ), and allowable bearing capacity ( $Q_a$ ) in **Tables 3, 4 and 5**, within the distinct Opolo geological layers 1, 2, and 3. These alterations are visually represented using the Kriging method, a geostatistical technique employed for comprehensive analysis. **Figure 8**, on the other hand, specifically presents the competent site suitability map for foundation sites, encompassing topsoil (layer 1), as well as layers 2 and 3, and employs the index overlay method. This method involves assigning score values based on multiple criteria as per established geotechnical standards (as detailed in **Tables 1 and 2**). These criteria consider factors such as oedometric modulus ( $E_c$ ), N-value, ultimate bearing capacity ( $Q_{ult}$ ), and allowable bearing capacity ( $Q_a$ ), which are also illustrated in **Figures 5, 6, and 7**. The resultant maps serve the purpose of identifying areas competent for foundation construction. Within **Figure 8**, the regions shaded in red signify zones unsuitable for foundation construction due to their geological incompetence. Yellow areas represent reasonably competent regions, while light blue areas indicate a higher level of competence, and blue areas are deemed highly competent for foundation purposes. This assessment is applicable within a depth range of 0.89 meters to 1.48 meters. Consequently, the red areas are deemed unsuitable for foundation construction, primarily due to their geological characteristics. Moving on to the second geological layer, the red regions now exhibit a level of competence, while yellow areas indicate competence, and blue areas signify a high level of competence for shallow foundation applications, typically at depths ranging from 1.52 meters to 3.84 meters. This analysis allows for informed decision-making regarding the suitability of the geological layers for different types of foundation construction. Furthermore, the third geological layer, as displayed in **Figure 8**, highlights areas of competence (yellow) and high competence

(blue) suitable for deep foundation applications, generally exceeding a depth of 3 meters. This geotechnical evaluation serves as a valuable resource for engineers and geologists to identify areas within the Opolo geological layers that are well-suited for the specific requirements of shallow and deep foundation construction projects.

### **Implications**

The implications of this research are significant for construction and geotechnical engineering in Opolo, Yenagoa, Bayelsa State, Nigeria. The utilization of near-surface seismic refraction surveys, combined with the Generalized Reciprocal Method (GRM), has provided valuable insights into the geotechnical characteristics of the study area. Firstly, the identification of three distinct geoseismic layers underscores the importance of a detailed geotechnical investigation before construction projects. It allows for a comprehensive understanding of the subsurface conditions, which is crucial for designing foundations that can safely support the intended structural loads. The findings regarding the first layer's unsuitability for supporting substantial structural loads have immediate practical implications. Builders and developers in Opolo need to be aware of this soft and weak alluvial deposit layer, which could pose challenges to construction projects. This knowledge can help avoid costly construction failures and ensure the safety and stability of structures. Conversely, the positive geotechnical parameters of the second layer make it a promising option for construction. The higher ultimate and allowable bearing capacities suggest that this layer can support a wide range of construction loads. This information is valuable for architects and engineers when planning and designing buildings and infrastructure in Opolo. Furthermore, the geographic information system (GIS) analysis provides a spatial perspective on the suitability of different areas within Opolo. It highlights variations in soil competence, which can guide site selection for specific projects and inform decisions about foundation types and construction techniques.

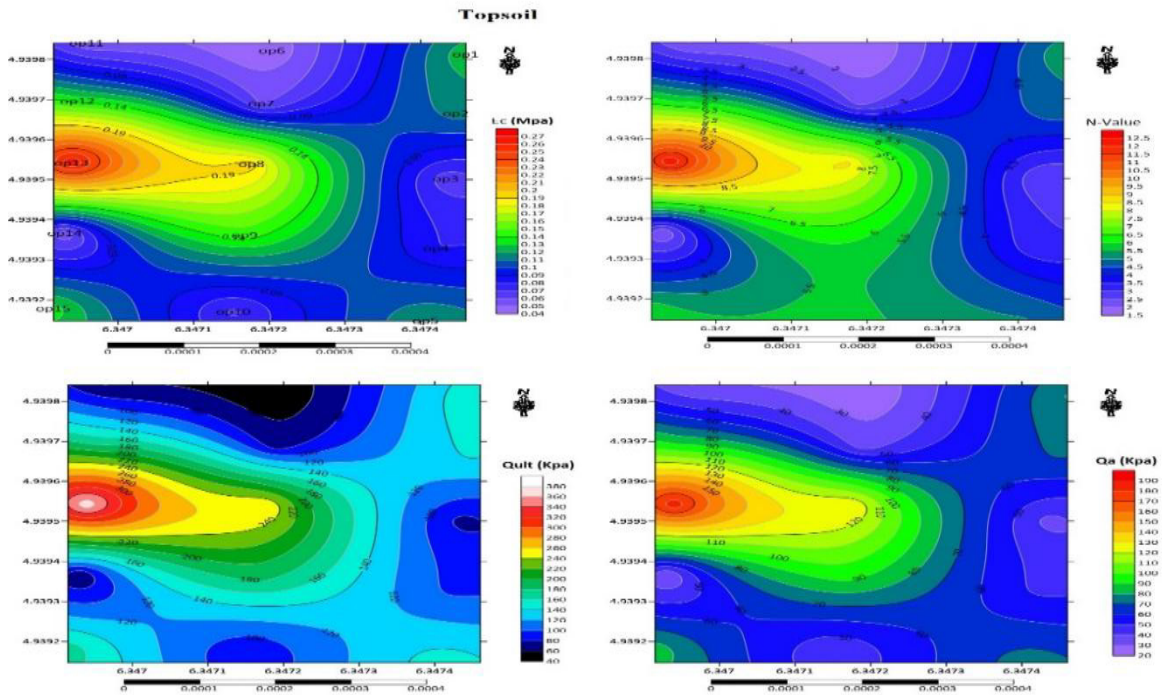


Figure 5. Distribution map of oedometric modulus ( $E_c$ ), N-value, ultimate bearing capacity ( $Q_{ult}$ ) and allowable bearing capacity ( $Q_a$ ) for topsoil Opolo.

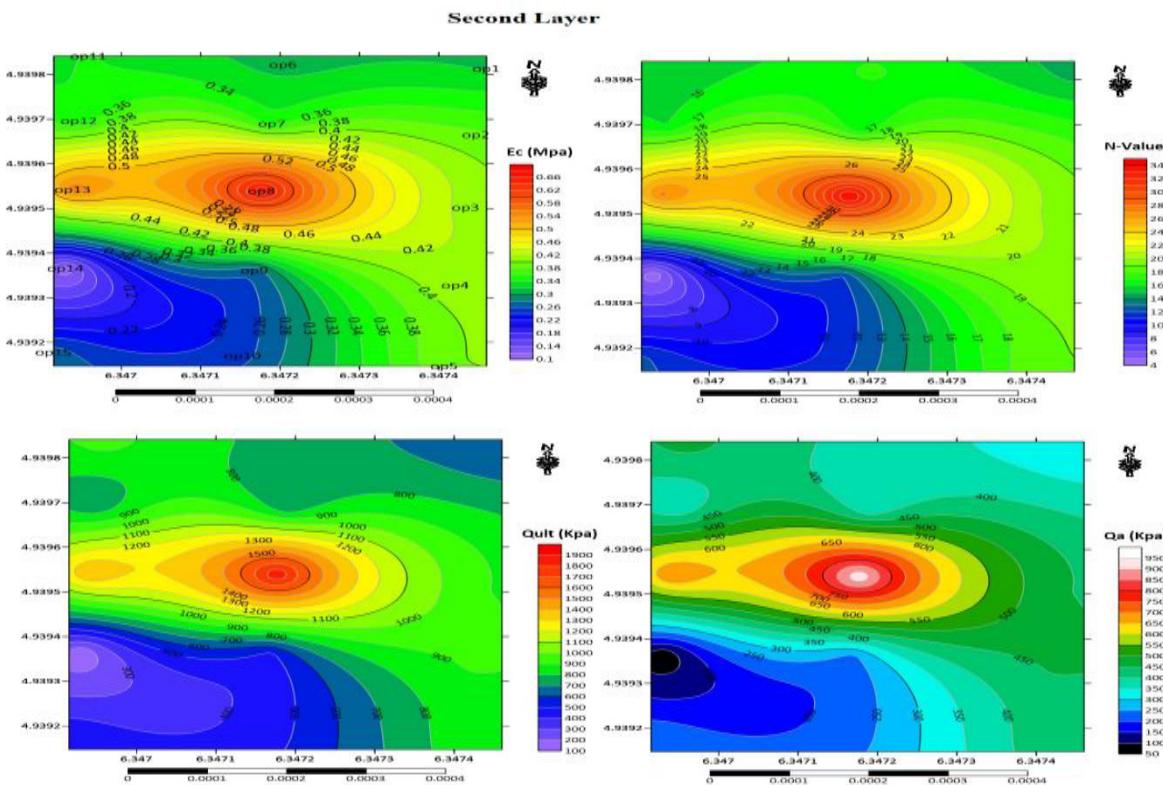


Figure 6. Distribution map of oedometric modulus ( $E_c$ ), N-value, ultimate bearing capacity ( $Q_{ult}$ ) and allowable bearing capacity ( $Q_a$ ) for second layer Opolo.

Third Layer

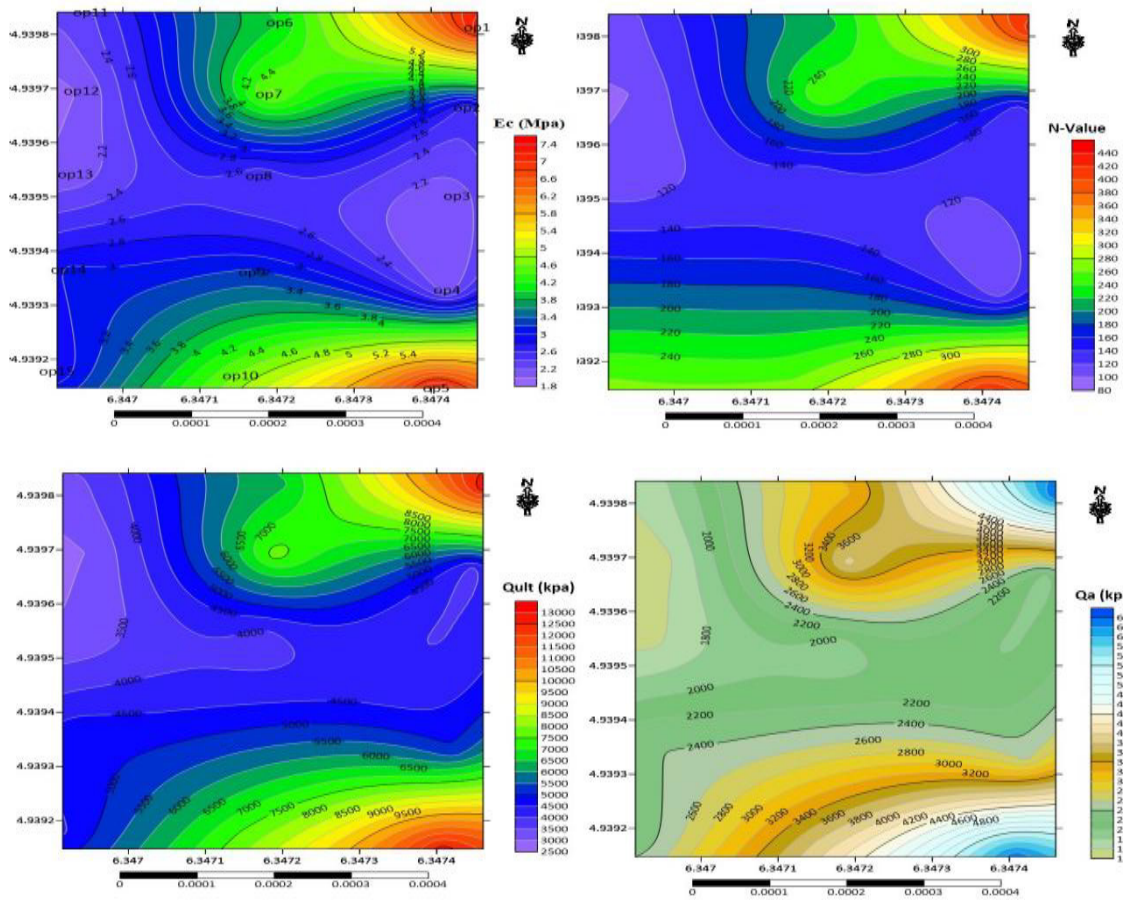


Figure 7. Distribution map of oedometer modulus (Ec), N-value, ultimate bearing capacity (Qult) and allowable bearing capacity (Qa) for third layer Opolo.

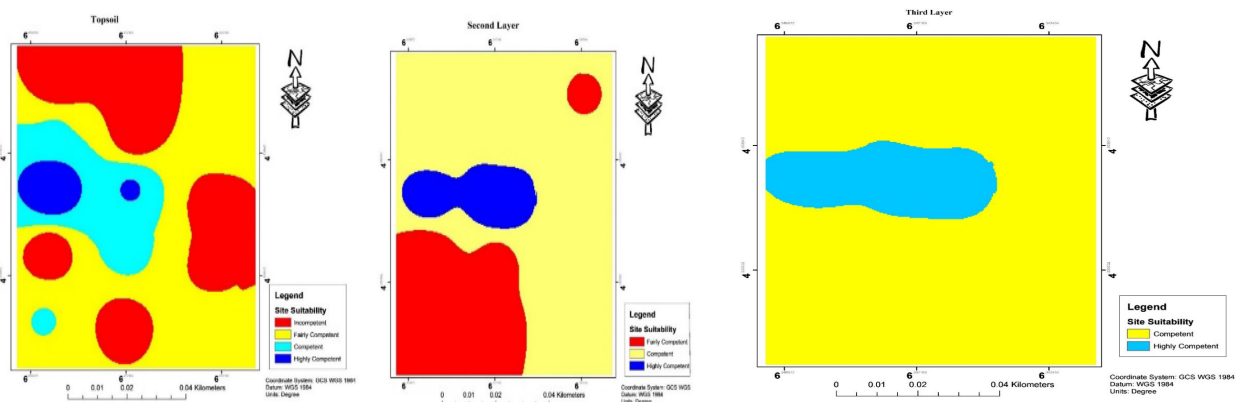


Figure 8. Competent site suitability maps from topsoil to third layer in Opolo study area.

## 4. Conclusions and recommendations

### 4.1 Conclusions

This research illustrates the utilization of near-surface seismic refraction surveys to establish crucial geotechnical parameters for soil characterization in potential construction locations. The study was carried out in Opolo, Yenagoa, Bayelsa State, Nigeria, involving the implementation of seismic profiling along three designated lines. Through meticulous analysis, three distinct geoseismic layers were identified, and their geotechnical properties were subsequently assessed using the Generalized Reciprocal Method (GRM). The initial layer, ranging from 0.89 meters to 1.50 meters in depth, exhibited notably low compressional and shear wave velocities, measuring between 178.17 to 264.40 meters per second and 104.83 to 155.50 meters per second, respectively. Correspondingly, this layer displayed low values for oedometric modulus, shear modulus, N-value, ultimate bearing capacity, and allowable bearing capacity. These characteristics collectively point to the presence of soft and weak alluvial deposits, rendering this layer unsuitable for supporting substantial structural loads. In contrast, the second layer, spanning from 1.52 meters to 3.84 meters in depth, presented significantly improved geotechnical parameters. It showcased notable values for ultimate and allowable bearing capacities, measuring between 460.15 to 716.80 kilopascals and 230.08 to 358.40 kilopascals, respectively. These findings indicate that the second layer can adequately support various construction loads. The third layer, extending from 15.00 meters to 26.05 meters in depth, exhibited variable thickness, ranging from 12.62 meters to 21.00 meters, and displayed moderately to competently compacted characteristics. Geographic Information System (GIS) analysis, employing the index overlay method, revealed that the top layer generally possesses fairly competent properties, with pockets of incompetency observed along the peripheries in Opolo. Conversely, the second and third layers at Opolo demonstrated fairly competent attributes, rendering them suitable for shallow footing and foundation design consid-

erations. However, it is crucial to note that the first layer is deemed unsuitable for construction due to its inherent incompetency.

### 4.2 Recommendations

Based on the geotechnical findings, it is advisable to exercise caution when selecting construction sites in Opolo, Yenagoa, Bayelsa State. Avoid building on the initial layer due to its inadequate bearing capacity. Opt for the second and third layers, which exhibit competent properties, especially for shallow footing and foundation designs. Further site-specific assessments and engineering solutions should be considered for safe and sustainable construction in Opolo.

### Author Contributions

O.E. developed the study with part of the writing and Formatting, E.D. processed the data and also assisted with writing. The final version was co-written by all authors.

### Conflict of Interest

There is no conflict of interest.

### References

- [1] Rowland, E., Ejaita, E., Omietimi, E.J., 2020. Foundation materials bearing capacity of Tombia Yenagoa, Bayelsa State Nigeria using multichannel analysis surface waves method. *International Journal of Advance Research and Innovative Ideas in Education*. 6(5), 811-823.
- [2] Omonefe, F., Desmond, E., Ebiegberi, O., et al., 2019. Analysis of near surface seismic refraction for geotechnical parameters in Opolo, Yenagoa of Bayelsa State. *Journal of Engineering Research and Reports*. 4(4), 1-12.
- [3] Roy, S., Bhalla, S.K., 2017. Role of geotechnical properties of soil on civil engineering structures. *Resources and Environment*. 7(4), 103-109.
- [4] Nouwakpo, S.K., Huang, C.H., 2012. A fluidized bed technique for estimating soil critical shear stress. *Soil Science Society of America*

- Journal. 76(4), 1192-1196.
- [5] Nwankwoala, H.O., Warmate, T., 2014. Geotechnical assessment of foundation conditions of a site in Ubima, Ikwerre local government area, Rivers State, Nigeria. *International Journal of Engineering Research and Development (IJERD)*. 9(8), 50-63.
- [6] Akintorinwa, O.J., Oluwole, S.T., 2018. Empirical relationship between electrical resistivity and geotechnical parameters: A case study of Federal University of Technology campus, Akure SW, Nigeria. *NRIAG Journal of Astronomy and Geophysics*. 7(1), 123-133.
- [7] Akinlabi, I.A., Adeyemi, G.O., 2014. Determination of empirical relations between geoelectrical data and geotechnical parameters in foundation studies for a proposed earth dam. *Pascal Journal Science Technology*. 15(2), 279-287.
- [8] Zhu, J., Wright, G., Wang, J., et al., 2018. A critical review of the integration of geographic information system and building information modelling at the data level. *ISPRS International Journal of Geo-Information*. 7(2), 66.
- [9] Bill, R., Blankenbach, J., Breunig, M., et al., 2022. Geospatial information research: State of the art, case studies and future perspectives. *PFG—Journal of Photogrammetry, Remote Sensing and Geoinformation Science*. 90(4), 349-389.  
DOI: <https://doi.org/10.1007/s41064-022-00217-9>
- [10] Palmer, D., 1980. The generalized reciprocal method of seismic refraction interpretation. *Society Exploration Geophysics*: London.
- [11] Mohamed, A.M., Abu El Ata, A.S.A., Abdel Azim, F., et al., 2013. Site-specific shear wave velocity investigation for geotechnical engineering applications using seismic refraction and 2D multi-channel analysis of surface waves. *NRIAG Journal of Astronomy and Geophysics*. 2(1), 88-101.
- [12] Imaitor-Uku, E.E., Owei, O.B., Hart, L., et al., 2021. Impact of settlement growth on Yenagoa's urban environment. *European Journal of Environment and Earth Sciences*. 2(1), 24-29.
- [13] Asare, E.N., Klu, A.K., 2019. The use of seismic refraction and geotechnical parameters to conduct site investigation—A case study. *International Journal of Advanced Engineering Research and Science*. 6(9).  
DOI: <https://doi.org/10.22161/ijaers.69.36>
- [14] Adewoyin, O.O., Joshua, E.O., Akinyemi, M.L., et al., 2021. Engineering site investigations using surface seismic refraction technique. *IOP Conference Series: Earth and Environmental Science*. 655(1), 012098.  
DOI: <https://doi.org/10.1088/1755-1315/655/1/012098>
- [15] Yilmaz, O., 2001. *Seismic data analysis: Processing, inversion, and interpretation of seismic data*. Society of Exploration Geophysicists: Tulsa, OK.
- [16] Khalil, M.H., Hanafy, S.M., 2008. Engineering applications of seismic refraction method: A field example at Wadi Wardan, Northeast Gulf of Suez, Sinai, Egypt. *Journal of Applied Geophysics*. 65(3-4), 132-141.  
DOI: <https://doi.org/10.1016/j.jappgeo.2008.06.003>
- [17] Mageshkumar, P., Subbaiyan, A., Lakshmanan, E., et al., 2019. Application of geospatial techniques in delineating groundwater potential zones: A case study from South India. *Arabian Journal of Geosciences*. 12, 1-15.
- [18] Kearey, P., Brooks, M., Hill, I., 2002. *An introduction to geophysical exploration*, third edition. Blackwell: London.
- [19] Lowrie, W., 2007. *Fundamentals of geophysics*, second edition. Cambridge University Press: Cambridge.
- [20] Reynolds, J.M., 2011. *An introduction to applied and environmental geophysics*. John Wiley & Sons: Hoboken.
- [21] Telford, W.M., Geldart, L.P., Sheriff, R.E., 1990. *Applied geophysics*. Cambridge University Press: Cambridge.
- [22] Atat, J.G., Akpabio, I.O., George, N.J., 2013. Allowable bearing capacity for shallow foundation in Eket local government area, Akwa Ibom State, southern Nigeria. *International Journal of*

- Geosciences. 4, 1491-1500.
- [23] Tezcan, S.S., Ozdemir, Z., Keceli, A., 2009. Seismic technique to determine the allowable bearing pressure for shallow foundations in soils and rocks. *Acta Geophysica*. 57, 400-412.
- [24] Essien, U.E., Akankpo, A.O., 2013. Compressional and shear-wave velocity measurements in unconsolidated top-soil in Eket, South-Eastern Nigeria. *The Pacific Journal of Science and Technology*. 14(1), 476-491.
- [25] Hassan, M., 2023. *Avantgarde reliability implications in civil engineering*. IntechOpen: London.  
DOI: <https://doi.org/10.5772/intechopen.102292>
- [26] Essien, U.E., Igboekwe, M.U., Akankpo, A.O., 2016. Determination of incompressibility, elasticity and rigidity of surface soils and shallow sediments from seismic wave velocities. *Journal of Earth Sciences and Geotechnical Engineering*. 6(1), 99-111.
- [27] Farauta, B.K., Egbule, C.L., Agwu, A.E., et al., 2012. Farmers' adaptation initiatives to the impact of climate change on agriculture in northern Nigeria. *Journal of Agricultural Extension*. 16(1), 132-144.  
DOI: <https://doi.org/10.4314/jae.v16i1.13>
- [28] Imai, T., Fumoto, H., Yokota, K., 1976. P- and S-wave velocities in subsurface layers of ground in Japan. *Urawa Research Institute*: Tokyo.
- [29] Stümpel, H., Kähler, S., Meissner, R., et al., 1984. The use of seismic shear waves and compressional waves for lithological problems of shallow sediments. *Geophysical Prospecting*. 32(4), 662-675.
- [30] Parry, R.H., 1977. Estimating bearing capacity in sand from SPT values. *Journal of the Geotechnical Engineering Division*. 103(9), 1014-1019.
- [31] Abd El-Rahman, M., 1991. The potential of absorption coefficient and seismic quality factor in delineating less sound foundation materials in Jabal Shib Az Sahara area, Northwest of Sanaa, Yemen Arab Republic. *Egypt, MERC Earth Science*. 5, 181-187.
- [32] Clark, S.P., 1966. *Handbook of physical constants*. Geological Society of America: Boulder, Colorado, U.S.
- [33] Gassman, F., 1973. *Seismische prospektion (German) [Seismic prospection]*. Birkhaeuser Verlag: Stuttgart. pp. 417.
- [34] Tatham, R.H., 1982. Vp Vs and lithology. *Geophysics*. 47(3), 336-344.
- [35] Sheriff, R.E., Geldart, L.P., 1986. *Exploration seismology*. Cambridge University Press: Cambridge.
- [36] Abd El-Rahman, M.A.H.D.Y., 1989. Evaluation of the kinetic elastic moduli of the surface materials and application to engineering geologic maps at Maba-Risabah area (Dhamar Province), Northern Yemen. *Egypt Journal Geology*. 33(1-2), 229-250.
- [37] Nwankwoala, H.O., Amadi, A.N., 2013. Geotechnical investigation of sub-soil and rock characteristics in parts of Shiroro-Muya-Chanchaga area of Niger State, Nigeria. *International Journal of Environmental and Engineering*. 6(1), 8-17.